

Tellurium-Bridged Manganese Carbonyl Clusters: Synthesis and Structural Transformations of $[\text{Te}_4\text{Mn}_3(\text{CO})_{10}]^-$, $[\text{Te}_2\text{Mn}_3(\text{CO})_9]^{2-}$, $[\text{Te}_2\text{Mn}_3(\text{CO})_9]^-$, and $[\text{Te}_2\text{Mn}_4(\text{CO})_{12}]^{2-}$

Minghuey Shieh,* Horng-Sun Chen, Huey-Yea Yang, Shu-Fen Lin, and Chuen-Her Ueng^[a]

Abstract: The reactions of appropriate ratios of K_2TeO_3 and $[\text{Mn}_2(\text{CO})_{10}]$ in superheated methanol solutions lead to a series of novel cluster anions $[\text{Te}_4\text{Mn}_3(\text{CO})_{10}]^-$ (**1**), $[\text{Te}_2\text{Mn}_3(\text{CO})_9]^{2-}$ (**2**), $[\text{Te}_2\text{Mn}_3(\text{CO})_9]^-$ (**3**), and $[\text{Te}_2\text{Mn}_4(\text{CO})_{12}]^{2-}$ (**4**). When cluster **1** is treated with $[\text{Mn}_2(\text{CO})_{10}]/\text{KOH}$ in methanol, paramagnetic cluster **2** is formed in moderate yield. Cluster **2** is oxidized by $[\text{Cu}(\text{MeCN})_4]\text{BF}_4$ to give the *closo*-clus-

ter $[\text{Te}_2\text{Mn}_3(\text{CO})_9]^-$ (**3**), while treatment of **2** with $[\text{Mn}_2(\text{CO})_{10}]/\text{KOH}$ affords the *closo*-cluster **4**. IR spectroscopy showed that cluster **1** reacted with $[\text{Mn}_2(\text{CO})_{10}]$ to give cluster **4** via cluster **2**. Clusters **1–4** were structurally characterized by

Keywords: bridging ligands • carbonyl ligands • cluster compounds • manganese • tellurium

spectroscopic methods or/and X-ray analyses. The core structure of **1** can be described as two $[\text{Mn}(\text{CO})_3]$ groups doubly bridged by two Te_2 fragments in a $\mu_2-\eta^2$ fashion. Both $[\text{Mn}(\text{CO})_3]$ groups are further coordinated to one $[\text{Mn}(\text{CO})_4]$ moiety. Cluster **2** is a 49 e^- species with a square-pyramidal core geometry. While cluster **3** displays a trigonal-bipyramidal metal core, cluster **4** possesses an octahedral core geometry.

Introduction

Whereas chalcogen-containing iron carbonyl clusters have been extensively investigated,^[1, 2] manganese carbonyl chalcogenide clusters are less well known, mainly because of the lack of rational synthetic routes. Compared to sulfur- and selenium-bridged manganese carbonyl clusters,^[3, 4, 5] the tellurium-bridged manganese carbonyl clusters are even more poorly explored.^[1] As to the tellurium-bridged manganese carbonyl complexes, a unique series of complexes $[\{\text{CpMn}(\text{CO})_2\}_2\text{Te}]$ and $[\{\text{Cp}^*\text{Mn}(\text{CO})_2\}_2\text{Te}]$ has been prepared in which the central tellurium atom displays multiple bonding to more than one metal center.^[6] Vahrenkamp et al. used organostannyl reagents to introduce tellurides into metal dimers to give $[\text{Mn}_2(\text{CO})_8(\mu\text{-TeSnMe}_3)_2]$.^[7] The tellurium-bridged dimanganese complex $[\text{Mn}_2(\text{Et}_3\text{P})_4(\text{CO})_6(\mu\text{-Te}_2)]$ was reported to be produced by the reaction of $[\text{Mn}_2(\text{CO})_{10}]$ and the tellurium-atom transfer reagent $\text{Et}_3\text{P}=\text{Te}$.^[8] Recently, the hydrothermal reaction of $[\text{Mn}_2(\text{CO})_{10}]$ with Na_2Te_2 and ethanol produced an anionic complex $[\text{Mn}_4(\text{CO})_{13}(\text{Te}_2)_3]^{2-}$ in which an $[\text{Mn}(\text{CO})_4]$ and three $[\text{Mn}(\text{CO})_3]$ fragments are bridged by three $[\text{Te}_2]^{2-}$ ligands.^[9] Nevertheless, no tellurium-

bridged manganese carbonyl clusters with Mn–Mn bonds were reported prior to our study.

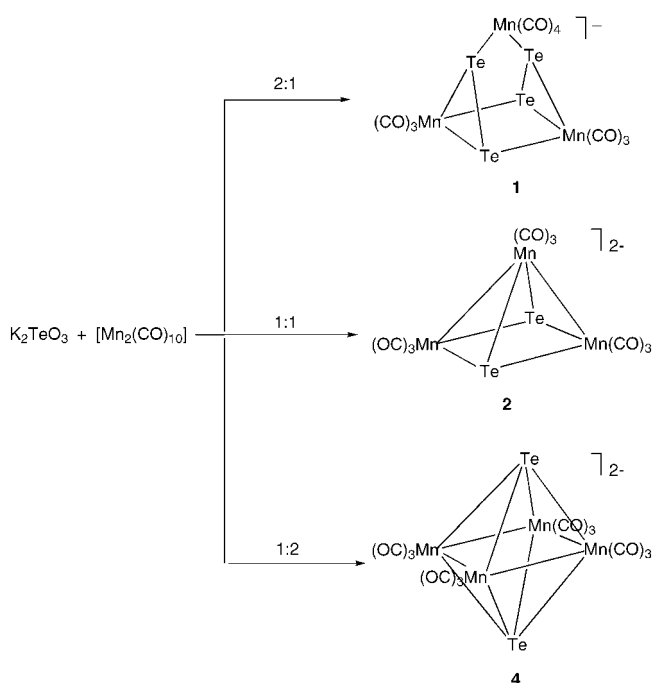
We have recently reported that the reaction of sulfur or selenium powder with dimanganese decacarbonyl in basic solutions leads to a series of sulfur- and selenium-bridged manganese carbonyl clusters.^[4] A similar methodology, however, was not applicable to the tellurium–manganese carbonyl system. Hence, the extension to the tellurium-containing manganese carbonyl system was full of interesting challenges. We report here the facile synthetic route to a new series of tellurium-bridged manganese carbonyl clusters $[\text{Te}_4\text{Mn}_3(\text{CO})_{10}]^-$ (**1**), $[\text{Te}_2\text{Mn}_3(\text{CO})_9]^{2-}$ (**2**), $[\text{Te}_2\text{Mn}_3(\text{CO})_9]^-$ (**3**), and $[\text{Te}_2\text{Mn}_4(\text{CO})_{12}]^{2-}$ (**4**) from K_2TeO_3 and $[\text{Mn}_2(\text{CO})_{10}]$ in *superheated MeOH solutions*. We have already communicated that cluster **4** can be metalated with $[\text{Me}_2\text{TeMn}(\text{CO})_4]^+$ to form the novel cluster $[\text{Me}_2\text{TeMn}(\text{CO})_4\text{Te}_2\text{Mn}_4(\text{CO})_{12}]^{2-}$ (**5**).^[10] Apart from the rare $\mu_5\text{-Te}$ bridging mode observed in cluster **5**, the $\mu_3, \eta^2\text{-Te}_2$, $\mu_3\text{-Te}$, and $\mu_4\text{-Te}$ bonding modes are found in clusters **1–4**. In addition, the structural relationships among these clusters are studied in depth along with their interesting structural transformations.

Results and Discussion

Syntheses of [TMBA][1], [PPN]₂[2], [PPN][3], and [PPN]₂[4]: We demonstrate here a direct and efficient route to a series of novel tellurium-bridged manganese carbonylates

[a] Prof. M. Shieh, H.-S. Chen, H.-Y. Yang, S.-F. Lin, Prof. C.-H. Ueng
Department of Chemistry
National Taiwan Normal University
Taipei 116, Taiwan, Republic of China
Fax: (+886)229-324249
E-mail: mshieh@sec.ntnu.edu.tw

that involves the direct thermal reactions of K_2TeO_3 with $[Mn_2(CO)_{10}]$ in superheated MeOH solutions. Depending on the ratio of K_2TeO_3 to $[Mn_2(CO)_{10}]$, this methodology leads to the formation of $[Te_4Mn_3(CO)_{10}]^-$ (**1**), $[Te_2Mn_3(CO)_9]^{2-}$ (**2**), and $[Te_2Mn_4(CO)_{12}]^{2-}$ (**4**) (Scheme 1). These anionic clusters



Scheme 1. Synthesis of **1**, **2** and **4** from K_2TeO_3 and $[Mn_2(CO)_{10}]$.

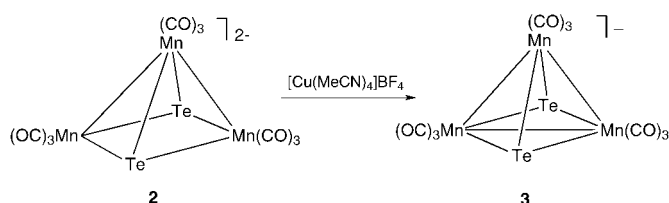
are quite reactive species; however, they can be isolated as the $[TMBA]^+$ (TMBA = benzyltrimethylammonium) salts or the $[PPN]^+$ (PPN = [bis(triphenylphosphane)iminium]) salts. Clusters **1**, **2**, and **4** are all fully characterized by spectroscopic methods and X-ray structural determination.

When K_2TeO_3 was treated with $[Mn_2(CO)_{10}]$ in a molar ratio of 2:1 in MeOH in a flask immersed in an oil bath at $110^\circ C$, the unusual cluster anion **1** resulted in moderate yield. The IR spectrum of $[TMBA][1]$ in the range $2059\text{--}1904\text{ cm}^{-1}$ shows

以不同比例之 K_2TeO_3 與 $Mn_2(CO)_{10}$ 在強熱的甲醇溶液中加熱迴流，成功的得到一新系列金屬團簇錯合物 $[Te_4Mn_3(CO)_{10}]^-$ (**1**)、 $[Te_2Mn_3(CO)_9]^{2-}$ (**2**)、 $[Te_2Mn_3(CO)_9]^-$ (**3**) 以及 $[Te_2Mn_4(CO)_{12}]^{2-}$ (**4**)。當化合物 **1** 與 $[Mn_2(CO)_{10}]/KOH$ 進一步反應，可得一順磁性產物—化合物 **2**，此化合物與 $[Cu(MeCN)_4][BF_4]$ 進行氧化反應，生成一閉環結構的化合物 **3**，而化合物 **4** 也可由化合物 **2** 與 $[Mn_2(CO)_{10}]/KOH$ 進行核擴充反應而得。另一方面，由 IR 光譜分析得知，化合物 **1** 與錳試劑反應則先形成化合物 **2**，再轉變為化合物 **4**。很幸運的，本文提及的化合物 **1-4** 皆有光譜分析與晶體繞射圖確認。首先，化合物 **1** 的主結構可視為兩個 $\mu_2\text{-}\eta^2$ 的 Te_2 配基橋接兩個 $Mn(CO)_3$ 片段，而另有一 $Mn(CO)_4$ 單元將 Te_2 配基連接形成籃子狀結構。其次，具有磁性的特殊化合物 **2**，主體為四角錐結構，而化合物 **3** 骨架則為雙三角錐。最後，化合物 **4** 則呈現八面體的對稱結構。本文提供有效且便利的合成方法，成功合成出一新系列的 Te-Mn-CO 金屬團簇化合物並對其結構作探討，而文中對化合物之間結構的轉變亦有深入的介紹。

characteristic absorptions of terminal carbonyl groups. An X-ray analysis shows that cluster **1** consists of a four-membered $[Te_2Mn_2]$ ring in which the two Te-Mn edges are each bridged by a Te atom that is further bonded to an apical $[Mn(CO)_4]$ fragment. If a molar ratio of 1:1 of K_2TeO_3 and $[Mn_2(CO)_{10}]$ is employed in the MeOH solution at $110^\circ C$, the square-pyramidal cluster anion **2** was obtained. On the other hand, when K_2TeO_3 was treated with $[Mn_2(CO)_{10}]$ in a molar ratio of 1:2 in the MeOH solution at $110^\circ C$, the octahedral cluster anion **4** was formed in good yield. Cluster **4** obeys Wade's rule for a six-vertex *closo*-cluster containing seven skeletal pairs and is stable in air for quite some time.

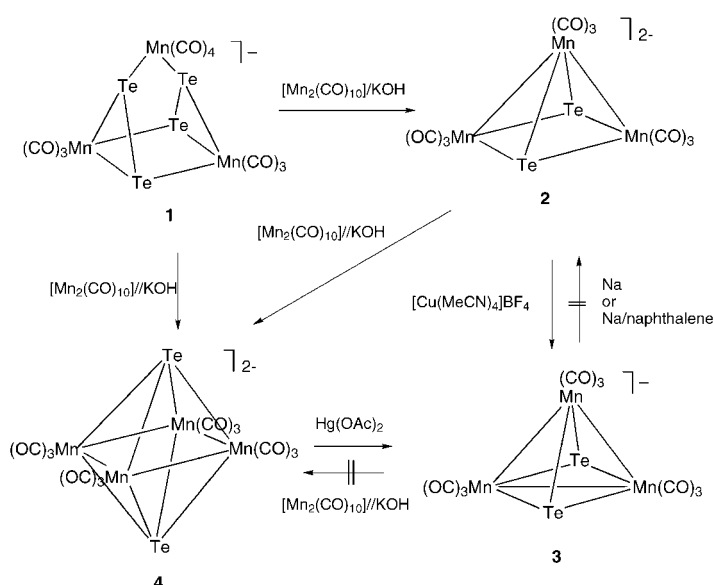
The clusters **1**, **2**, and **4** were formed by the reaction of K_2TeO_3 and $[Mn_2(CO)_{10}]$ in superheated MeOH solutions, in which reactions are facilitated by the elimination of CO_2 . The conditions for these reactions are critical: the outcome depends on the ratios of the reactants, reaction temperature, and reaction time, signifying that the variations of activation energies versus reaction time and ratios of reactants in this Te-Mn-CO system are decisive. The optimized conditions for these clusters are described in the Experimental Section. Cluster **2** is a 49-electron species and its paramagnetic behavior is confirmed by its powder EPR spectrum at room temperature in which $g = 2.49$. Based on electron counting, cluster **2** falls one electron short of that of a trimanganese cluster with two Mn-Mn bonds. Cluster **2** is very sensitive to the air on account of its electron deficiency. When the paramagnetic cluster **2** is carefully oxidized with $[Cu(MeCN)_4]BF_4$, a trigonal-bipyramidal cluster anion $[Te_2Mn_3(CO)_9]^-$ (**3**) is obtained (Scheme 2). Cluster **3** is a 48-electron species, which is in agreement with conventional electron counting.



Scheme 2. Reaction of **2** with $[Cu(MeCN)_4]BF_4$ to give **3**.

Note that cluster **3** cannot be obtained directly from the thermal reaction of K_2TeO_3 with $[Mn_2(CO)_{10}]$ under similar conditions, but it can be produced in good yield from the oxidation of **2** by the oxidizing agent $[Cu(MeCN)_4]BF_4$. Although the analogous trigonal-bipyramidal cluster $[Se_2Mn_3(CO)_9]^-$ can be obtained from SeO_2 with $[Mn_2(CO)_{10}]/KOH$,^[4] a similar methodology which uses TeO_2 and $[Mn_2(CO)_{10}]/KOH$,^[11] failed to yield cluster **3**; this method gave mixtures of **2** and **4** which are difficult to separate. Compared with the direct thermal reactions of K_2TeO_3 with $[Mn_2(CO)_{10}]$ in MeOH described above, the disadvantages of the treatment of TeO_2 with $[Mn_2(CO)_{10}]/KOH/MeOH$ are difficult separations and highly basic conditions.

Transformations of $[TMBA][1]$, $[PPN]_2[2]$, $[PPN][3]$, and $[PPN]_2[4]$: The structural transformations of clusters **1-4** are summarized in Scheme 3. Since the ratio of K_2TeO_3 to



Scheme 3. Relationship between 1–4.

$[\text{Mn}_2(\text{CO})_{10}]$ affects the outcome of these reactions as well, it was investigated whether structural transformations of these tellurium–manganese carbonylates could be accomplished. Therefore, we conducted a series of experiments in which the ratio of K_2TeO_3 to dimanganese was varied: we found interesting cluster transformations in this system. It was discovered that cluster **1** reacted with the appropriate amount of $[\text{Mn}_2(\text{CO})_{10}]$ in basic solution to form cluster **2**. Furthermore, paramagnetic cluster **2** was converted to cluster **4** by treatment with $[\text{Mn}_2(\text{CO})_{10}]/\text{KOH}$ in methanol. Following a similar methodology, cluster **4** was formed directly from cluster

1 when **1** was treated with $[\text{Mn}_2(\text{CO})_{10}]/\text{KOH}$ in methanol. These results suggest that cluster **2** may represent the intermediate state for the transformation of **1** to the octahedral complexes **4**. In addition, cluster **4** is believed to undergo complicated bond breakage and formation to give cluster **3** upon the addition of the appropriate amount of $\text{Hg}(\text{OAc})_2$.

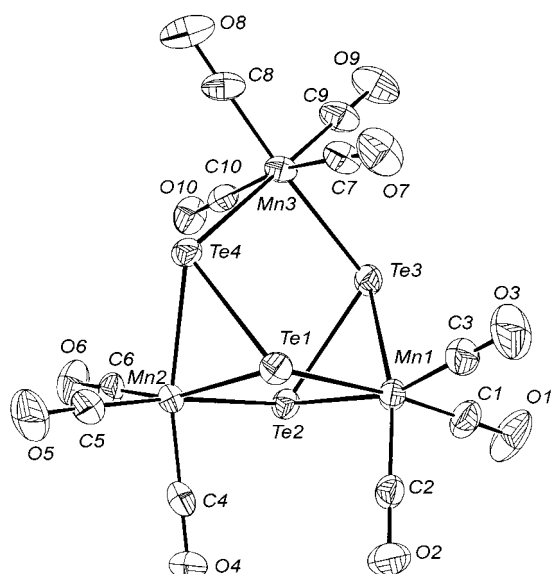
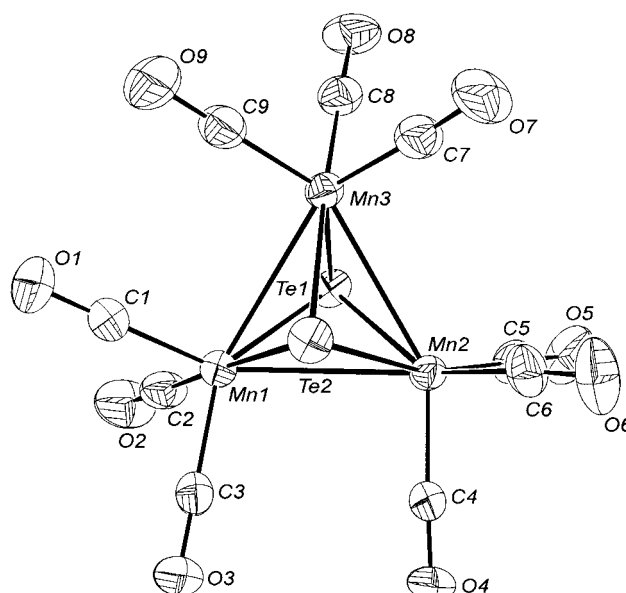
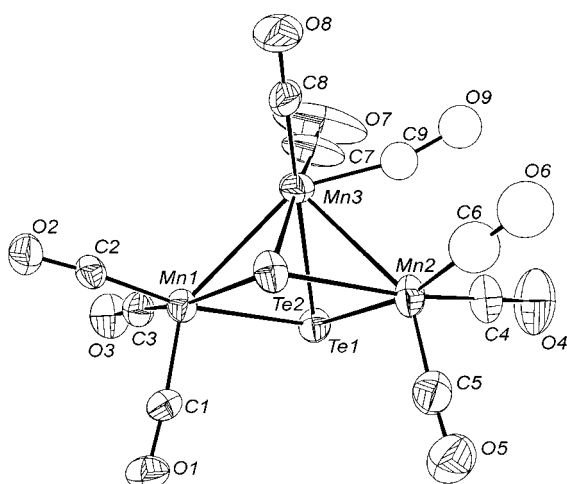
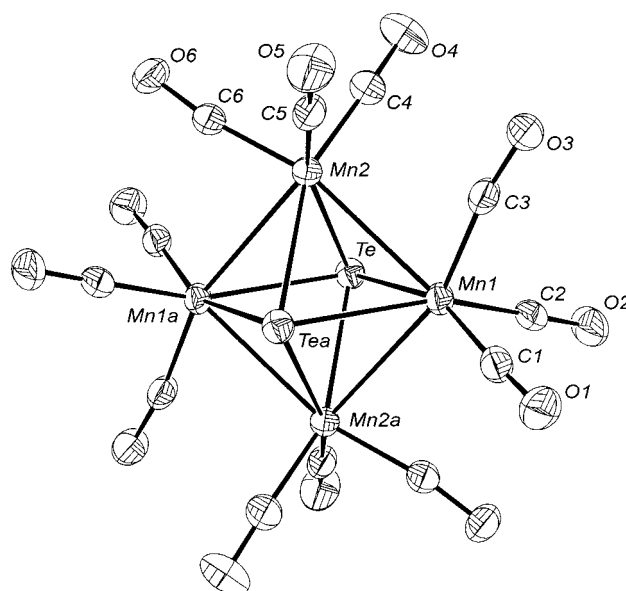
As mentioned above, cluster **3** is readily obtained from the mild oxidation of **2** with $[\text{Cu}(\text{MeCN})_4]\text{BF}_4$. It was of interest to know whether **3** can be reconverted back to cluster **2** by treatment with reducing agents. It was found that **3** remained intact on treatment with $\text{Na}/\text{naphthalene}$ or even with Na . This indicates a high degree of inertness of **3**. The cyclic voltammogram of **2** exhibits two reversible redox couples at $E_{1/2} = -391$ and -508 mV (100 mV s^{-1} , $\Delta E = 68$ and 83 mV, respectively) versus SCE. However, the electrochemical measurement of $[\text{PPN}][\mathbf{3}]$ only shows the irreducible oxidation of the cations, which is consistent with the inertness of **3** towards chemical reduction. This behavior is also evidenced by the fact that the trigonal-bipyramidal cluster **3** cannot undergo cluster expansion with $[\text{Mn}_2(\text{CO})_{10}]/\text{KOH}$ to form the octahedral cluster **4**, while the paramagnetic square-pyramidal cluster **2** does. Radical processes should account for the cluster expansion from **2** to **4**.

Structures of $[\text{TMBA}][\mathbf{1}]$, $[\text{PPN}]_2[\mathbf{2}] \cdot \text{CH}_2\text{Cl}_2$, $[\text{PPN}][\mathbf{3}]$, and $[\text{PPN}]_2[\mathbf{4}]$: The structures of $[\text{TMBA}][\mathbf{1}]$, $[\text{PPN}]_2[\mathbf{2}] \cdot \text{CH}_2\text{Cl}_2$, $[\text{PPN}][\mathbf{3}]$, and $[\text{PPN}]_2[\mathbf{4}]$ are depicted in Figures 1–4; selected bond lengths and angles are listed in Table 1.

The core structure of **1** can be described as two $[\text{Mn}(\text{CO})_3]$ groups doubly bridged by two Te_2 fragments in a $\mu_2-\eta^2$ fashion. These double are further bonded to a $[\text{Mn}(\text{CO})_4]$ moiety. The metal core of cluster **1** can be regarded as an inorganic analogue of the well-known quadricyclane. This

Table 1. Selected bond lengths [\AA] and bond angles [$^\circ$] for $[\text{TMBA}][\mathbf{1}]$, $[\text{PPN}]_2[\mathbf{2}] \cdot \text{CH}_2\text{Cl}_2$, $[\text{PPN}][\mathbf{3}]$, and $[\text{PPN}]_2[\mathbf{4}]$.

$[\text{TMBA}][\text{Te}_4\text{Mn}_3(\text{CO})_{10}]$ ($[\text{TMBA}][\mathbf{1}]$)									
Te1–Te4	2.733(1)	Te1–Mn1	2.654(1)	Te1–Mn2	2.670(1)	Te2–Te3	2.7205(7)	Te2–Mn1	2.663(1)
Te2–Mn2	2.645(1)	Te3–Mn1	2.649(1)	Te3–Mn3	2.632(1)	Te4–Mn2	2.641(1)	Te4–Mn3	2.642(1)
Te4–Te1–Mn1	107.45(3)	Te4–Te1–Mn2	58.51(3)	Mn1–Te1–Mn2	93.05(3)	Te3–Te2–Mn1	58.95(3)	Te3–Te2–Mn2	108.11(3)
Mn1–Te2–Mn2	93.41(4)	Te2–Te3–Mn1	59.44(3)	Te2–Te3–Mn3	108.16(3)	Mn1–Te3–Mn3	117.96(4)	Te1–Te4–Mn2	59.55(3)
Te1–Te4–Mn3	107.47(3)	Mn2–Te4–Mn3	118.69(3)	Te1–Mn1–Te2	86.29(3)	Te1–Mn1–Te3	98.57(4)	Te2–Mn1–Te3	61.61(3)
Te1–Mn2–Te2	86.29(3)	Te1–Mn2–Te4	61.94(3)	Te2–Mn2–Te4	98.23(3)	Te3–Mn3–Te4	95.21(3)		
$[\text{PPN}]_2[\text{Te}_2\text{Mn}_3(\text{CO})_9] \cdot \text{CH}_2\text{Cl}_2$ ($[\text{PPN}]_2[\mathbf{2}] \cdot \text{CH}_2\text{Cl}_2$)									
Te1–Mn1	2.607(2)	Te1–Mn2	2.613(2)	Te1–Mn3	2.627(2)	Te2–Mn1	2.612(2)	Te2–Mn2	2.615(2)
Te2–Mn3	2.625(2)	Mn1–Mn3	2.808(2)	Mn1–C9'	2.54(2)	Mn2–Mn3	2.791(2)	Mn2–C9	2.47(2)
Mn1–Te1–Mn2	97.43(5)	Mn1–Te1–Mn3	64.89(5)	Mn2–Te1–Mn3	64.32(5)	Mn1–Te2–Mn2	97.28(5)	Mn1–Te2–Mn3	64.86(5)
Mn2–Te2–Mn3	64.37(5)	Te1–Mn1–Te2	82.73(4)	Te1–Mn1–Mn3	57.89(4)	Te2–Mn1–Mn3	57.79(5)	Te1–Mn2–Te2	82.55(5)
Te1–Mn2–Mn3	58.06(5)	Te2–Mn2–Mn3	57.99(5)	Te1–Mn3–Te2	82.11(5)	Te1–Mn3–Mn1	57.22(4)	Te1–Mn3–Mn2	57.59(5)
Te2–Mn3–Mn1	57.35(4)	Te2–Mn3–Mn2	57.65(5)	Mn1–Mn3–Mn2	88.96(6)	Mn3–C9–O9	163.4(17)	Mn3–C9'–O9'	160.5(14)
$[\text{PPN}][\text{Te}_2\text{Mn}_3(\text{CO})_9]$ ($[\text{PPN}][\mathbf{3}]$)									
Te1–Mn1	2.505(1)	Te1–Mn2	2.535(1)	Te1–Mn3	2.512(1)	Te2–Mn1	2.548(2)	Te2–Mn2	2.554(1)
Te2–Mn3	2.567(1)	Mn1–Mn2	2.933(2)	Mn1–Mn3	2.919(1)	Mn2–Mn3	2.903(2)		
Mn1–Te1–Mn2	71.18(4)	Mn1–Te1–Mn3	71.16(4)	Mn2–Te1–Mn3	70.25(4)	Mn1–Te2–Mn2	70.18(4)	Mn1–Te2–Mn3	69.60(4)
Mn2–Te2–Mn3	69.09(4)	Mn2–Mn1–Mn3	59.50(4)	Mn1–Mn2–Mn3	60.01(3)	Mn1–Mn3–Mn2	60.49(4)		
$[\text{PPN}]_2[\text{Te}_2\text{Mn}_4(\text{CO})_{12}]$ ($[\text{PPN}]_2[\mathbf{4}]$)									
Te–Mn1	2.6363(8)	Te–Mn1a	2.6360(6)	Te–Mn2	2.6487(8)	Te–Mn2a	2.6446(7)	Mn1–Tea	2.6360(6)
Mn1–Mn2	2.7979(8)	Mn1–Mn2a	2.8241(9)	Mn2–Tea	2.6446(7)	Mn1–Te–Mn1a	97.42(2)	Mn1–Te–Mn2	63.93(2)
Mn1–Te–Mn2a	64.66(2)	Mn1a–Te–Mn2	64.60(2)	Mn1a–Te–Mn2a	63.99(2)	Mn2–Te–Mn2a	97.82(2)	Te–Mn1–Tea	82.58(2)
Te–Mn1–Mn2	58.25(2)								
Te–Mn1–Mn2a	57.82(2)	Tea–Mn1–Mn2	58.15(2)	Tea–Mn1–Mn2a	57.92(2)	Mn2–Mn1–Mn2a	90.40(2)	Te–Mn2–Tea	82.18(2)
Te–Mn2–Mn1	57.82(2)	Te–Mn2–Mn1a	57.48(2)	Tea–Mn2–Mn(1)	57.86(2)	Tea–Mn2–Mn1a	57.53(2)	Mn1–Mn2–Mn1a	89.60(3)

Figure 1. Structure of anion **1** (ORTEP diagram; 30% thermal ellipsoids).Figure 3. Structure of anion **3** (ORTEP diagram; 30% thermal ellipsoids).Figure 2. Structure of dianion **2** (ORTEP diagram; 30% thermal ellipsoids).Figure 4. Structure of dianion **4** (ORTEP diagram; 30% thermal ellipsoids).

cluster is structurally similar to the recently reported $[\text{CrFe}_2(\text{CO})_{10}\text{Se}_4]$ cluster.^[12] In **1**, each $\mu_3\text{-Te}_2$ unit can be considered as a six-electron donor to the core framework to make cluster **1** a 54-electron species, in agreement with the effective atomic number (EAN) rule. The Te–Te bond length of 2.742 Å is close to those in $[\text{M}(\text{CO})_4\text{Te}_4]^{2-}$ (2.724 Å, M = Cr; 2.729 Å, M = Mo),^[13] $[\text{Cr}_4(\text{CO})_{20}(\text{Te}_2)]^{2-}$ (2.784 Å),^[14] and $[\{\text{Cr}(\text{CO})_5\}_2\text{-Te}_2]^{2-}$ (2.736 Å);^[15] however, it is shorter than those in $[(\text{W}(\text{CO})_3)_6(\text{Te}_2)_4]^{2-}$ (2.852 Å)^[16] and $\{\text{Cr}(\text{CO})_5\}_4\text{Te}_4$ (2.856 Å).^[17]

Cluster **2** has a square-pyramidal core geometry in which the Mn_3 unit is doubly bridged by the $\mu_3\text{-Te}$ atoms. This complex is analogous to the recently reported cluster $[\text{Se}_2\text{Mn}_3(\text{CO})_9]^{2-}$,^[3] which is a paramagnetic 49-electron cluster. Cluster **3** has a trigonal-bipyramidal Te_2Mn_3 core in which the Mn_3 plane is capped above and below by the $\mu_3\text{-Te}$ atoms. Cluster **4** displays a near-idealized octahedral framework with four Mn–Mn bonds of similar lengths (2.7979–2.8241 Å) and nearly perfect internal Mn–Mn–Mn angles

(89.60–90.40°), in which the four Mn atoms are capped by two $\mu_4\text{-Te}$ atoms and are each seven-coordinate. For comparison, the average Te–Mn and Mn–Mn bond lengths in clusters **1–4** and other related clusters are listed in Table 2.

Semibridging carbonyls in $[\text{PPN}]_2[\mathbf{2}] \cdot \text{CH}_2\text{Cl}_2$ and $[\text{PPN}]_2[\mathbf{4}]$:

As shown in Figure 2, there are two conformational molecules of **2** in the crystal lattice, each of which possesses a semibridging carbonyl group C9–O9 or C9'–O9' lying on the opposite sides of the Mn_3 atom and the semibridging carbonyl C9–O9 and C9'–O9' and are each present with 50% probability. The disorder of C7 and O7 cannot be resolved and is covered with large thermal parameters. Similar to that in the case of $[\text{Se}_2\text{Mn}_3(\text{CO})_9]^{2-}$,^[3] cluster **2** possesses a semibridging carbonyl group^[18] that has some interaction with the

Table 2. Average Te–Mn and Mn–Mn bond lengths [\AA] in clusters **1–4** and other related clusters.

Compound	Te–Mn	Mn–Mn
$[\text{Mn}_4\text{Te}_4(\text{SC}_3\text{H}_7)_4]^{4+}$ ^[23]	2.782	
$[\text{Mn}_4\text{Te}_4(\text{SeC}_3\text{H}_7)_4]^{4+}$ ^[23]	2.769	
$[\text{Mn}_4\text{Te}_4(\text{TeC}_3\text{H}_7)_4]^{4+}$ ^[24]	2.740	
$[(\text{Et}_3\text{P})_2(\text{CO})_3\text{MnTe}]_2$ ^[8]	2.718	
[TMBA][1] ^[a]	2.645	
$[\text{PPN}]_2[\text{2}] \cdot \text{CH}_2\text{Cl}_2$ ^[a]	2.617	2.799
[PPN][3] ^[a]	2.537	2.918
[PPN] ₂ [4] ^[a]	2.641	2.811

[a] This work.

basal Mn2 and Mn1 with significant bending of carbonyl group (Mn3–C9–O9 163.4°; Mn3–C9'–O9' 160.5°) and the distances between Mn2/C9 and Mn1/C9' are 2.47(2) and 2.54(2) \AA , respectively. Since these two conformational molecules of **2** are in a 1:1 superposition, the semibridging carbonyl can be considered to interact with only one basal Mn atom. If each tellurium atom can be formally assigned a -2 oxidation state, the oxidation state of the apical Mn3 should be $+1$, while the basal Mn2 and Mn1 atom are in the 0 or $+1$ oxidation state, respectively.

Interestingly, in cluster **4**, there appear to be four weak interactions between the carbonyls and Mn1 and Mn2 atoms, as evidenced by the shorter distances between Mn2/C3 and Mn1a/C6 (2.793(3) and 2.864(3) \AA , respectively) and the slight bending of the carbonyl group (Mn1–C3–O3 171.2(3)°, Mn2–C6–O6 171.2(3)°). These carbonyls (C3–O3, C3'–O3', C6–O6, and C6'–O6') can also be considered to be semibridging carbonyls according to the suggestion made by Curtis.^[18]

Conclusion

We have demonstrated the facile syntheses of a series of tellurium-bridged manganese carbonyl clusters that exhibit novel structural features. We have also established some cornerstones for further study in this rarely explored area. The interesting structural transformations in this system are studied systematically; they suggest that it is possible to introduce other metal fragments for further cluster growth.

Experimental Section

All reactions were performed under an atmosphere of pure nitrogen in standard Schlenk glassware and by the use of Schlenk techniques.^[19] Solvents were purified, dried, and distilled under nitrogen prior to use. $[\text{Mn}_2(\text{CO})_{10}]$ (Strem), TeO_2 (Strem), $\text{K}_2\text{TeO}_3 \cdot \text{H}_2\text{O}$ (Aldrich), [PPN]Cl (Aldrich), and [TMBA]Cl (Aldrich), were used as received. IR spectra were recorded on a Jasco 5300 or a Perkin-Elmer paragon 500 IR spectrometer as solutions in CaF_2 cells. Elemental analyses of C, H, and N were performed on a Perkin-Elmer 2400 analyzer at the NSC Regional Instrumental Center at National Taiwan University, Taipei (Taiwan).

Synthesis of [TMBA][Te₄Mn₃(CO)₁₀] ([TMBA][1]): MeOH (40 mL) was added to a mixture of $[\text{Mn}_2(\text{CO})_{10}]$ (0.687 g, 1.762 mmol) and $\text{K}_2\text{TeO}_3 \cdot \text{H}_2\text{O}$ (1.193 g, 4.389 mmol). The mixed solution was refluxed in an oil bath at 110 °C for 24 h. The reddish-brown solution was filtered and concentrated, and an aqueous solution of [TMBA]Cl (0.401 g, 2.159 mmol) was added.

The precipitated solid was washed with deionized water several times and then extracted into CH_2Cl_2 . The CH_2Cl_2 extract was recrystallized from CH_2Cl_2 /hexanes to give [TMBA][1] (0.858 g, 0.77 mmol; 70% based on Te). IR (CH_2Cl_2): $\tilde{\nu}_{\text{CO}} = 2059$ (w), 1990 (vs), 1974 (s), 1953 (w), 1904 (s) cm^{-1} ; elemental analysis (%) calcd for [TMBA][Te₄Mn₃(CO)₁₀]: C 21.73, H 1.46, N 1.27; found: C 22.15, H 1.48, N 1.20. The complex is soluble in diethyl ether, CH_2Cl_2 , THF, MeOH, and MeCN. The reddish black crystals suitable for X-ray analysis were grown from a diethyl ether solution.

Synthesis of [PPN]₂[Te₂Mn₃(CO)₉] ([PPN]₂[2]): MeOH (40 mL) was added to a mixture of $[\text{Mn}_2(\text{CO})_{10}]$ (0.845 g, 2.17 mmol) and $\text{K}_2\text{TeO}_3 \cdot \text{H}_2\text{O}$ (0.550 g, 2.167 mmol). The mixed solution was refluxed in an oil bath at 110 °C for 72 h. The brownish-green solution was filtered and concentrated, and a MeOH solution of [PPN]Cl (1.25 g, 2.18 mmol) was added dropwise. The precipitated solid was washed with MeOH several times. The residue dissolved in CH_2Cl_2 (15 mL) and diethyl ether (7.5 mL) was added to the solution to remove the impurities, and the filtrate was dried under vacuum and recrystallized with CH_2Cl_2 /diethyl ether several times to give [PPN]₂[Te₂Mn₃(CO)₉] (1.38 g, 1.69 mmol; 73% based on Te). IR (CH_2Cl_2): $\tilde{\nu}_{\text{CO}} = 1983$ (m), 1940 (s), 1881 (m), 1865 (m) cm^{-1} ; elemental analysis (%) calcd for [PPN]₂[Te₂Mn₃(CO)₉] $\cdot \text{CH}_2\text{Cl}_2$: C 53.70, H 3.41, N 1.53; found: C 53.47, H 3.43, N 1.60. [PPN]₂[2] is soluble in CH_2Cl_2 , THF, and MeCN, slightly soluble in MeOH, but insoluble in hexanes and diethyl ether. The brownish black crystals suitable for X-ray analysis were grown from a CH_2Cl_2 /diethyl ether solution.

Synthesis of [PPN]₂[Te₂Mn₄(CO)₁₂] ([PPN]₂[4]): MeOH (40 mL) was added to a mixture of $[\text{Mn}_2(\text{CO})_{10}]$ (0.725 g, 1.86 mmol) and $\text{K}_2\text{TeO}_3 \cdot \text{H}_2\text{O}$ (0.236 g, 0.930 mmol). The mixed solution was refluxed in an oil bath at 110 °C for 98 h. The deep-brown solution was filtered and concentrated, and a MeOH solution of [PPN]Cl (0.705 g, 1.23 mmol) was added dropwise. The precipitated solid was washed with deionized water several times. The residue was recrystallized with CH_2Cl_2 /MeOH several times to give [PPN]₂[Te₂Mn₄(CO)₁₂] (0.44 g, 0.233 mmol; 50% based on Te). IR (CH_2Cl_2): $\tilde{\nu}_{\text{CO}} = 1941$ (s), 1884 (m) cm^{-1} ; elemental analysis (%) calcd for [PPN]₂[Te₂Mn₄(CO)₁₂]: C 53.43, H 3.20, N 1.48; found: C 53.44, H 3.15, N 1.47. [PPN]₂[4] is soluble in CH_2Cl_2 , THF, and MeCN, but insoluble in hexanes, diethyl ether, and MeOH. The purple-black crystals suitable for X-ray analysis were grown from a MeCN solution.

Synthesis of [PPN][Te₂Mn₃(CO)₉] ([PPN][3])

Method 1: CH_2Cl_2 (30 mL) was added to a mixture of [PPN]₂[2] (0.40 g, 0.229 mmol) and $[\text{Cu}(\text{MeCN})_4]\text{BF}_4$ (0.057 g, 0.181 mmol). The mixed solution was refluxed in an oil bath at 70–80 °C for 68 h. The brown solution was filtered and the solvent was removed under vacuum. The residue was washed with hexanes and extracted with Et_2O to give [PPN]₂[3] (0.14 g, 0.116 mmol; 51% based on [PPN]₂[2]). IR (CH_2Cl_2): $\tilde{\nu}_{\text{CO}} = 1996$ (s), 1912 (m), 1881 (m), 1865 (m) cm^{-1} ; elemental analysis (%) calcd for [PPN][Te₂Mn₃(CO)₉]: C 44.10, H 2.55, N 1.20; found: C 44.64, H 2.50, N 1.16. [PPN]₂[3] is soluble in CH_2Cl_2 and Et_2O . The deep-brown crystals suitable for X-ray analysis were grown from a CH_2Cl_2 solution.

Method 2: To a solution of [PPN]₂[4] (0.59 g; 0.312 mmol) in CH_2Cl_2 (20 mL) in an ice-water bath was added $\text{Hg}(\text{OAc})_2$ (0.11 g, 0.345 mmol). The mixed solution was turned from purple to brownish, which was filtered and solvent was removed under vacuum. The residue was washed with hexanes and extracted with Et_2O to give [PPN]₂[3] (0.24 g, 0.198 mmol; 63% based on [PPN]₂[4]).

Reaction of [TMBA][Te₄Mn₃(CO)₁₀] ([TMBA][1]) with $[\text{Mn}_2(\text{CO})_{10}]$ /KOH: MeOH (40 mL) was added to a mixture of [TMBA][1] (0.441 g, 0.399 mmol), $[\text{Mn}_2(\text{CO})_{10}]$ (0.195 g (0.500 mmol), and KOH (0.898 g, 16.0 mmol). The mixed solution was refluxed in an oil bath at 110 °C for 48 h. The brownish green solution was filtered and concentrated, and a MeOH solution of [PPN]Cl (0.918 g, 1.60 mmol) was added dropwise. The precipitated solid was washed with MeOH several times. The residue was recrystallized with $\text{Et}_2\text{O}/\text{CH}_2\text{Cl}_2$ twice to give [PPN]₂[2] (0.75 g, 0.429 mmol; 63% based on Te).

Reaction of [PPN]₂[Te₂Mn₃(CO)₉] ([PPN]₂[2]) with $[\text{Mn}_2(\text{CO})_{10}]$ /KOH: MeOH (20 mL) and MeCN (20 mL) were added to a mixture of [PPN]₂[2] (0.504 g, 0.288 mmol), $[\text{Mn}_2(\text{CO})_{10}]$ (0.124 g, 0.318 mmol), and KOH (0.326 g, 5.81 mmol). The mixed solution was refluxed in an oil bath at 110 °C for 30 h. The brown solution was filtered and solvent was removed under vacuum. The residue was extracted with CH_2Cl_2 and the CH_2Cl_2

extract was recrystallized from Et₂O/CH₂Cl₂ to give [PPN]₂[4] (0.130 g, 0.069 mmol; 24% based on [PPN]₂[2]).

Cyclic voltammetry measurements of [PPN]₂[2]·CH₂Cl₂ and [PPN][3]: Cyclic voltammetry experiments were performed with BAS100B/W. Solutions were prepared in dried CH₂Cl₂ with tetra-*n*-butylammonium perchlorate (TBAP, 0.1M), recrystallized before use as the supporting electrolyte. A three-electrode configuration was used with a platinum disk working electrode, a platinum wire auxiliary electrode, and Ag/AgO reference electrode. The redox potentials were calibrated with a ferrocene/ferrocene (Fc⁺/Fc) couple in the working solution. Experiments were carried out at room temperature under nitrogen.

X-ray structural characterization of complexes [TMBA][1], [PPN]₂[2]·CH₂Cl₂, [PPN][3], and [PPN]₂[4]: Selected crystallographic data for [TMBA][1], [PPN]₂[2]·CH₂Cl₂, [PPN][3], and [PPN]₂[4] are given in Table 3. Data collection was carried out with a Nonius CAD-4 diffractometer that used graphite-monochromated MoK_α radiation at 25 °C and a $\theta/2\theta$ scan mode. A ψ scan absorption correction carried out.^[20] All crystals were mounted on glass fibers with epoxy cement. Data reduction and structural refinement were performed with the NRCC-SDP-VAX packages,^[21] and atomic scattering factors were taken from International Tables for X-ray Crystallography.^[22]

Structures of [TMBA][1], [PPN]₂[2]·CH₂Cl₂, [PPN][3], and [PPN]₂[4]: Cell parameters were obtained from 25 reflections with 2θ angle in the range 22.42–32.72° for [TMBA][1], 16.68° < 2θ < 29.34° for [PPN]₂[2]·CH₂Cl₂, 22.94 < 2θ < 28.66° for [PPN][3], and 22.84 < 2θ < 31.42° for [PPN]₂[4]. A total of 3697 reflections with $I > 2.5\sigma(I)$ for [TMBA][1] (6761 reflections with $I > 2.5\sigma(I)$ for [PPN]₂[2]·CH₂Cl₂, 5333 reflections with $I > 2.5\sigma(I)$ for [PPN][3], and 5885 reflections with $I > 2.5\sigma(I)$ for [PPN]₂[4]) were refined by least-squares cycles. All the non-hydrogen atoms were refined with anisotropic temperature factors, except those for [PPN]₂[2]·CH₂Cl₂, C6, O6, C9, O9, C9', and O9' which were refined with isotropic temperature factors. Full-matrix least-squares refinement led to convergence with $R = 0.027$ and $R_w = 0.026$ for [TMBA][1], with $R = 0.043$ and $R_w = 0.036$ for [PPN]₂[2]·CH₂Cl₂, with $R = 0.033$ and $R_w = 0.026$ for [PPN][3], and with $R = 0.026$ and $R_w = 0.022$ for [PPN]₂[4].

Crystallographic data (excluding structure factors) for the structures of [TMBA][1], [PPN]₂[2]·CH₂Cl₂, and [PPN][3] reported in this paper have been deposited with the Cambridge Crystallographic Data Centre as supplementary publication nos. CCDC-154903 ([TMBA][1]), CCDC-154902 ([PPN]₂[2]·CH₂Cl₂), and CCDC-154901 ([PPN][3]). Copies of the data can be obtained free of charge on application to CCDC, 12 Union Road, Cambridge CB2 1EZ, UK (fax: (+44) 1223-336-033; e-mail: deposit@ccdc.cam.ac.uk). Further details of the crystal structure investigation of [PPN]₂[4] may be obtained from the Fachinformationszentrum Karlsruhe,

76344 Eggenstein-Leopoldshafen (Germany), (Fax: (+49) 7247-808-666; e-mail: crysdata@fiz.karlsruhe.de) on quoting the depositary number CSD-408889 ([PPN]₂[4]).

Acknowledgement

We thank the National Science Council of the Republic of China for financial support (NSC 89–2113-M-003–031).

- a) W. A. Herrmann, *Angew. Chem.* **1986**, *98*, 57; *Angew. Chem. Int. Ed. Engl.* **1986**, *25*, 56; b) N. A. Compton, R. J. Errington, N. C. Norman, *Adv. Organomet. Chem.* **1990**, *100*, 223; c) L. Linford, H. G. Raubenheimer, *Adv. Organomet. Chem.* **1991**, *32*, 1; d) D. Fenske, J. Ohmer, J. Hachgenei, K. Merzweiler, *Angew. Chem.* **1988**, *100*, 1300; *Angew. Chem. Int. Ed. Engl.* **1988**, *27*, 1277; e) L. C. Roof, J. W. Kolis, *Chem. Rev.* **1993**, *93*, 1037; f) R. D. Adams, *Polyhedron* **1985**, *4*, 2003; g) L. E. Bogan, T. B. Rauchfuss, A. L. Rheingold, *J. Am. Chem. Soc.* **1985**, *107*, 3843; h) K. H. Whitmire, *J. Coord. Chem.* **1988**, *17*, 95; i) P. Mathur, *Adv. Organomet. Chem.* **1997**, *41*, 243; j) M. Shieh, *J. Clust. Sci.* **1999**, *10*, 3.
- The Chemistry of Metal Cluster Complexes* (Eds.: D. F. Shriver, H. D. Kaesz, R. D. Adams), VCH, New York, **1990**.
- R. Seidel, B. Schnautz, G. Henkel, *Angew. Chem.* **1996**, *108*, 1836; *Angew. Chem. Int. Ed. Engl.* **1996**, *35*, 1710.
- K.-C. Huang, Y.-C. Tsai, G.-H. Lee, S.-M. Peng, M. Shieh, *Inorg. Chem.* **1997**, *36*, 4421.
- Z. G. Fang, T. S. A. Hor, K. F. Mok, S.-C. Ng, L.-K. Liu, Y.-S. Wen *Organometallics* **1993**, *12*, 1009.
- a) M. Herberhold, D. Reiner, D. Neugebauer, *Angew. Chem.* **1983**, *95*, 46; *Angew. Chem. Int. Ed. Engl.* **1983**, *22*, 59; b) W. A. Herrmann, C. Hecht, M. L. Ziegler, B. Balbach, *J. Chem. Soc. Chem. Commun.* **1984**, 686.
- V. Küllmer, H. Vahrenkamp, *Chem. Ber.* **1977**, *110*, 228.
- M. L. Steigerwald, C. E. Rice, *J. Am. Chem. Soc.* **1988**, *110*, 4228.
- S. D. Huang, C. P. Lai, C. L. Barnes, *Angew. Chem.* **1997**, *109*, 1961; *Angew. Chem. Int. Ed. Engl.* **1997**, *36*, 1854.
- M. Shieh, H.-S. Chen, H.-Y. Yang, C.-H. Ueng, *Angew. Chem.* **1999**, *111*, 1339; *Angew. Chem. Int. Ed. Engl.* **1999**, *38*, 1252.
- W. Schatz, H.-P. Neumann, B. Nuber, B. Kanellakopoulos, M. L. Ziegler, *Chem. Ber.* **1991**, *124*, 453.
- P. Mathur, P. Sekar, *Organometallics* **1997**, *16*, 142.

Table 3. Crystallographic data for [TMBA][Te₄Mn₃(CO)₁₀] ([TMBA][1]), [PPN]₂[Te₂Mn₃(CO)₉]·CH₂Cl₂ ([PPN]₂[2]·CH₂Cl₂), [PPN][Te₂Mn₃(CO)₉] ([PPN][3]), and [PPN]₂[Te₂Mn₄(CO)₁₂] ([PPN]₂[4]).

	[TMBA][1]	[PPN] ₂ [2]·CH ₂ Cl ₂	[PPN][3]	[PPN] ₂ [4]
empirical formula	C ₂₀ H ₁₆ Mn ₃ NO ₁₀ Te ₄	C ₈₂ H ₆₂ Cl ₂ Mn ₃ N ₂ O ₉ P ₄ Te ₂	C ₄₅ H ₃₀ Mn ₃ NO ₉ P ₂ Te ₂	C ₈₄ H ₆₀ Mn ₄ N ₂ O ₁₂ P ₄ Te ₂
fw	1105.55	1834.20	1210.68	1888.23
crystal dimensions [mm]	0.40 × 0.45 × 0.50	0.35 × 0.25 × 0.12	0.50 × 0.45 × 0.30	0.50 × 0.45 × 0.41
space group	<i>P</i> $\bar{1}$	<i>P</i> $\bar{1}$	<i>P</i> ₂ / <i>c</i>	<i>P</i> $\bar{1}$
<i>a</i> [Å]	10.232(1)	13.762(2)	16.900(6)	12.200(2)
<i>b</i> [Å]	13.146(2)	13.871(2)	17.680(6)	13.158(3)
<i>c</i> [Å]	14.236(2)	24.333(4)	17.475(5)	13.791(2)
α [°]	101.43(1)	79.82(2)		66.96(2)
β [°]	109.14(1)	80.97(2)	117.38(3)	89.63(2)
γ [°]	112.05(1)	61.19(1)		77.46(2)
<i>V</i> [Å ³]	1559.7(4)	3992(1)	4636(3)	1981.0(6)
<i>Z</i>	2	2	4	1
ρ_{calcd} [g cm ⁻³]	2.354	1.526	1.734	1.583
μ (MoK α) [cm ⁻¹]	49.1	13.9	21.6	14.9
λ [Å]	0.7107	0.7107	0.7107	0.7107
<i>T</i> [°C]	25	25	25	25
<i>R</i> ^[a] , <i>R</i> _w ^[b]	0.027, 0.026	0.045, 0.037	0.033, 0.026	0.026, 0.022

[a] $R = \sum |F_o - F_c| / \sum F_o$. [b] $R_w = [\sum w(F_o - F_c)^2 / \sum w(F_o)^2]^{1/2}$.

- [13] W. A. Flomer, S. C. O'Neal, J. W. Kolis, D. Jeter, A. W. Cordes, *Inorg. Chem.* **1988**, *27*, 969.
- [14] L. C. Roof, W. T. Pennington, J. W. Kolis, *Inorg. Chem.* **1992**, *31*, 2056.
- [15] S. Stauf, C. Reisner, W. Tremel, *Chem. Commun.* **1996**, 1749.
- [16] L. C. Roof, W. T. Pennington, J. W. Kolis, *J. Am. Chem. Soc.* **1990**, *112*, 8172.
- [17] O. Blacque, H. Brunner, M. M. Kubicki, B. Nuber, B. Stubenhofer, J. Wachter, B. Wrackmeyer, *Angew. Chem.* **1997**, *109*, 361; *Angew. Chem. Int. Ed. Engl.* **1997**, *36*, 352.
- [18] M. D. Curtis, K. R. Han, W. M. Butler, *Inorg. Chem.* **1980**, *19*, 2096.
- [19] D. F. Shriver, M. A. Drezzon, *The Manipulation of Air Sensitive Compounds*; Wiley, New York, **1986**.
- [20] A. C. T. North, D. C. Philips, F. S. Mathews, *Acta Crystallogr.* **1968**, *A24*, 351.
- [21] E. J. Gabe, Y. Le Page, J. P. Charland, F. L. Lee, P. S. White, *J. Appl. Crystallogr.* **1989**, *22*, 384.
- [22] *International Tables for X-ray Crystallography; Vol. IV*, Kynoch press, Birmingham, England, **1974**.
- [23] H.-O. Stephan, G. Henkel, *Angew. Chem.* **1994**, *106*, 2422; *Angew. Chem. Int. Ed. Engl.* **1994**, *33*, 2322.
- [24] H.-O. Stephan, C. Chen, G. Henkel, K. Greesar, W. Haase, *J. Chem. Soc. Chem. Commun.* **1993**, 886.

Received: January 3, 2001 [F2983]